WL-TR-96-7046

Synthesis and Thermal Properties of 1,3-Dinitro-3-(1',3'-dinitroazetidin-3'-yl) azetidine (TNDAZ) and Its Admixtures with TNAZ

Robert L. McKenney, Jr.
Thomas G. Floyd
William E. Stevens

Wright Laboratory, Armament Directorate
Munitions Division
Energetic Materials Branch
Eglin AFB FL 32542-5910

Alan P. Marchand
G. V. M. Sharma
Simon G. Bott

Department of Chemistry
University of North Texas
Denton TX 76203-0068

Thomas G. Archibald
Aerojet, Propulsion Division
PO Box 13222
Sacramento CA 95813-6000

July 1996

INTERIM REPORT FOR PERIOD OCTOBER 1994 - May 1996

APPROVED FOR PUBLIC RELEASE-DISTRIBUTION UNLIMITED

WRIGHT LABORATORY, ARMAMENT DIRECTORATE
Air Force Materiel Command ■ United States Air Force ■ Eglin Air Force Base

19960903 067

DTIC QUALITY INSPECTED 1

NOTICE

When Government drawings, specifications, or other data are used for any purpose other than in connection with a definitely Government-related procurement, the United States Government incurs no responsibility or any obligation whatsoever. The fact that the Government may have formulated or in any way supplied the said drawings, specifications, or other data, is not to be regarded by implication, or otherwise as in any manner construed, as licensing the holder, or any other person or corporation; or as conveying any rights or permission to manufacture, use or sell any patented invention that may in any way be related thereto.

This report has been reviewed and is approved for publication.

FOR THE COMMANDER

AARON D. BRINSON
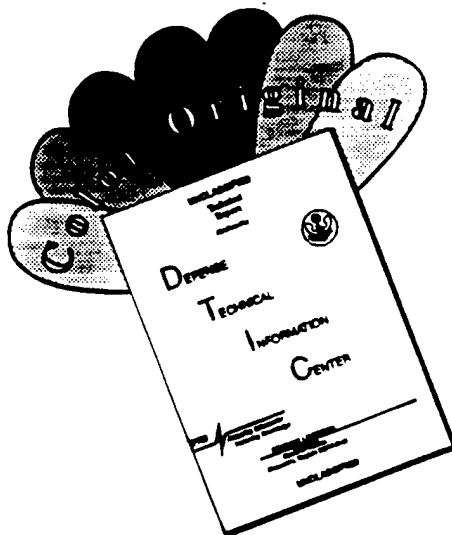Technical Director, Munitions Division

Even though this report may contain special release rights held by the controlling office, please do not request copies from the Wright Laboratory/Armament Directorate. If you qualify as a recipient, release approval will be obtained from the originating activity by DTIC. Address your request for additional copies to:

Defense Technical Information Center
8725 John J. Kingman Road
Ft Belvoir VA 22060-6218

If your address has changed, if you wish to be removed from our mailing list, or if your organization no longer employs the addressee, please notify WL/MNME, 2306 Perimeter Rd. Ste 9, Eglin AFB FL 32542-5910, to help us maintain a current mailing list.

Do not return copies of this report unless contractual obligations or notice on a specific document requires that it be returned.

DISCLAIMER NOTICE

REPORT DOCUMENTATION PAGE

1. AGENCY USE ONLY *(Leave blank)*	2. REPORT DATE July 1996	3. REPORT TYPE AND DATES COVERED Final, October 1994- May 1996

4. TITLE AND SUBTITLE
Synthesis and Thermal Properties of 1,3-Dinitro-3-(1',3'-dinitroazetidin-3'-yl) azetidine (**TNDAZ**) and Its Admixtures with **TNAZ**.

6. AUTHOR(S)
Robert L. Mckenney, Jr., Thomas G. Floyd, William E. Stevens, Alan P. Marchand, G. V. M. Sharma, S. G. Bott and T. G. Archibald

5. FUNDING NUMBERS

PE: 62602F
PR: 2502
TA: 10
WU: 22

7. PERFORMING ORGANIZATION NAME(S) AND ADDRESS(ES)
Wright Laboratory, Armament Directorate
Munitions Division
Energetic Materials Branch (WL/MNME)
Eglin AFB FL 32542-5910

8. PERFORMING ORGANIZATION REPORT NUMBER

WL-TR-96-7046

9. SPONSORING/MONITORING AGENCY NAME(S) AND ADDRESS(ES)

Same as Block 7.

10. SPONSORING/MONITORING AGENCY REPORT NUMBER

11. SUPPLEMENTARY NOTES

Availability of this report is specified on verso of front cover.

12a. DISTRIBUTION/AVAILABILITY STATEMENT
Approved for public release; distribution is unlimited.

12b. DISTRIBUTION CODE

A

13. ABSTRACT *(Maximum 200 words)*
The synthesis of the title compound, **TNDAZ**, in four steps by starting with *N*-t-Butyl-3(hydroxymethyl)-3-nitroazetidine is described. The structures of **TNDAZ** and of a precursor, *N*-t-Butyl-3-nitro-3-(*N'*-t-butyl-3'-nitroazetidin-3'-yl)azetidine have been established unequivocally via application of single crystal X-ray crystallographic techniques. Thermal properties of **TNDAZ**, alone and in admixture with 1,3,3-trinitroazetidine (**TNAZ**). are presented. In particular, a binary phase diagram has been predicted computationally and confirmed experimentally using the techniques of differential scanning calorimetry and hot stage microscopy. Data support the existence of more than one polymorph for both **TNDAZ** and **TNAZ**.

14. SUBJECT TERM **TNDAZ, TNAZ**, Eutectic, Polymorph, Properties, Phase Diagram

15. NUMBER OF PAGES
48

16. PRICE CODE

17. SECURITY CLASSIFICATION OF REPORT UNCLASSIFIED	18. SECURITY CLASSIFICATION OF THIS PAGE UNCLASSIFIED	19. SECURITY CLASSIFICATION OF ABSTRACT UNCLASSIFIED	20. LIMITATION OF ABSTRACT None

PREFACE

TABLE OF CONTENTS

LIST OF FIGURES

LIST OF TABLES

SECTION I

INTRODUCTION

1. BACKGROUND

1,3,3-Trinitroazetidine (**TNAZ**), a novel energetic material that is of considerable interest to the Department of Defense, was first prepared by Archibald and co-workers in 1990 (Reference 1). In recent years, several research groups have turned their attention to developing improved methods for the synthesis of **TNAZ** (References 2-5). Although **TNAZ** is a powerful and thermally stable energetic material, its application to melt cast explosive formulations has been limited by its high volatility characteristics and its tendency to form low density castings at atmospheric pressure (Reference 6). The porosity resulting from the casting process using pure **TNAZ** appears to be evenly distributed throughout the charge. In an attempt to alter these unacceptable characteristics, researchers are endeavoring to form binary eutectic compositions with a variety of other energetic materials (Reference 7). The work presented in this technical report describes the synthesis and thermal characterization of 1,3-dinitro-3-(1',3'-dinitroacetidin-3'-yl)azetidine (**TNDAZ**) and its admixtures with **TNAZ**. It is anticipated that this structurally similar, yet less volatile, material will form a binary eutectic with **TNAZ** that will result in a composite explosive of overall reduced volatility and of acceptable charge quality and performance.

SECTION II

EXPERIMENTAL

1. GENERAL

All melting points are uncorrected.

2. STRUCTURAL CHARACTERIZATION

a. X-ray Structures of **TNDAZ** and *N-t*-**Butyl-3-nitro-3-(*N-t*-butyl-3'-nitroazetidin-3'-yl)azetidine (4)** (Reference 8a)

Data were collected on an Enraf-Nonius CAD-4 diffractometer by using the ω-20 scan technique, Mo Kα radiation ($\lambda = 0.71073$ Å) and a graphite monochromator. Standard procedures in our laboratory that have been described previously were used for this purpose (Reference 8b). Pertinent details are presented in Table 1. Data were connected for Lorentz and polarization effects but not for absorption. The structures were solved by direct methods (**TNDAZ** by MULTAN (Reference 9) and **4** by SHELXS86 (Reference 10), and the model was refined by using full-matrix least-squares techniques. The number of atoms treated with anisotropic thermal parameters depended upon the number of observed reflections. For **TNDAZ**, sufficient data were available to refine every non-hydrogen atom in this fashion. However, for **4**, all atoms were refined as isotropic. Hydrogen atoms were located on difference maps and then included in the model as found for **TNDAZ** and in idealized positions [U(H) = 1.3 B$_{eq}$(C)] for **4**. All computations other than those specified were performed by using *Mol*EN (Reference 10). Scattering factors were taken from the usual sources (Reference 11).

3. THERMAL CHARACTERIZATION

a. Differential Scanning Calorimetry (DSC)

Neat components, **TNAZ** and **TNDAZ**, and twenty-one **TNAZ/TNDAZ** mixtures were thermally characterized using a TA Instruments, Dual Differential Scanning Calorimeter, Model 912, equipped with a 2100 Thermal Analyzer Data System. Standard aluminum sample pans, Part No. 072492, were used for all melting operations. Lids, Part No. 073191, were inverted to eliminate/minimize free volume over the sample. To minimize the probability of component interaction in the mixtures and/or leakage from the sealed pans, an upper temperature limit of 105 °C was enforced , as well as a sample weight limitation of 1-2 mg. A minimum of three melting/cooling

operations were carried out for all samples at a heating rate of 5 °C/m. Mixtures were prepared by grinding weighed portions of dry **TNAZ** and **TNDAZ** in an agate mortar with a glass pestle to ensure homogeniety. The instrument was calibrated using Indium metal as a temperature standard.

b. Hot Stage Microscopy (HSM)

HSM experiments were carried out using a Mettler hot stage, Model FP 82, equipped with an FP 80 Central Processor. All observations were made with a Leitz Orthoplan Universal Largefield microscope equipped with a polarizing condenser and either a Polaroid PM-CP 3.25 x 4.25 camera or a high-resolution video system, Javelin Smart Camera, Model JE3762DSP operating at shutter speeds of 1/60 and 1/500 s. The lower power photomicrographs were taken through a Leitz NPL 10X 0.20P lens (150x) and those at higher power through a Leitz 170/0.17 NPL Fluotar 16/0.45 lens (240x).

c. High Performance Liquid Chromatography (HPLC)

TNDAZ and **TNAZ** were analyzed by HPLC using a Waters Millennium Chromatographic System equipped with a Waters 996 Photodiode Array detector and a C_{18} column. The mobile phase was a 60:40 acetonitrile:water mixture. All experiments were carried out at ambient temperature at a flow rate of 1.2 cm^3/m. Purity calculations were carried out using the area normalization method.

d. Modified Vacuum Thermal Stability Test (MVTS).

The MVTS test is used to determine the thermal stability of energetic materials/formulations that have been exposed to 100 °C for 48 h under an initial vacuum. The sample, 100 to 500 mg, is contained in a volume-calibrated stainless steel reaction vessel assembly that is connected to a pressure sensor. Other versions of the test are described in Reference 12. Both the reaction vessel and pressure sensor are maintained at the same temperature (100 °C) for the duration of the test. Real-time pressure/temperature data are recorded via a computerized data acquisition system. Total gas volume (cm^3) generated during the 48 hours is computed from the pressure/temperature data and supported by gas chromatographic analysis.

The gases generated/evolved during the MVTS test were analyzed using a Varian Gas Chromatograph, Model 3400. The instrument is equipped with a thermal conductivity detector and a 9 ft x 0.125 in stainless steel column packed with Porapak Q (100/200 mesh). The gases were flushed from the reaction vessel into the gas chromatograph with helium at a flow rate of 40 cm^3/m. The analysis program is initiated with an 8-minute hold at -98 °C followed by programmed heating to 200 °C at

a rate of 5 °C/m. Data are acquired and manipulated with a Hewlett Packard 3365 Series II ChemStation.

1. SYNTHESIS

a. *N-t*-Butyl-3-bromo-3-nitroazetidine (2)

To a stirred solution of NaOH (2.52 g, 63 mmol) in water (25 mL), was added portionwise *N-t*-Butyl-3-hydroxymethyl-3-nitroazetidine (1) (Reference 3) (5.64 g, 30 mmol), and the resulting mixture was allowed to stir at room temperature for 3 h. The reaction mixture then was cooled via external application of an ice-water bath, and bromine (1.6 mL, 31 mmol) was added dropwise with stirring. The reaction mixture was stirred for 1 h after all of the bromine had been added. The resulting mixture was filtered, and the residue was washed with water (100 mL). The residue was dissolved in CH_2Cl_2 (50 mL), and the resulting solution was washed successively with water (2 x 25 mL), 15 percent aqueous $Na_2S_2O_3$ (2 x 25 mL), and water (25 mL). The organic layer was dried (Na_2SO_4) and filtered, and the filtrate was concentrated *in vacuo*. The residue thereby obtained was purified via column chromatography on silica gel by eluting with 1:5 EtOAc-ligroin. Pure 2 (2.27 g, 32 percent) was thereby obtained as a pale yellow microcrystalline solid: mp 85-86 °C; IR (See Table A-1); ^1H NMR ($CDCl_3$) δ 0.95 (s, 9 H), 3.78 (AB, J_{AB} = 11.0 Hz, 2 H), 4.15 (AB, J_{AB} = 11.0 Hz, 2 H); ^{13}C NMR ($CDCl_3$) δ 24.45 (q), 52.96 (s), 61.77 (t), 76.64 (s). Anal Calcd for $C_7H_{13}BrN_2O_2$: C, 35.46; H, 5.52. Found: C, 35.50; H, 5.68.

b. *N-t*-Butyl-3-nitroazetidine (3)

To a solution of 2 (5.0 g, 21 mmol) in EtOH (180 mL) under nitrogen atmosphere at room temperature was added dropwise a solution of $NaBH_4$ (3.36 g, 88 mmol) in 60 % aqueous EtOH (90 mL). The resulting mixture was stirred at ambient temperature for 5 h and then was concentrated *in vacuo*. Water (60 mL) was added to the residue, and the resulting aqueous suspension was extracted with CH_2Cl_2 (3 x 40 mL). The organic layer was washed successively with water (3 x 50 mL) and brine (25 mL), dried (Na_2SO_4), and filtered, and the filtrate was concentrated *in vacuo*. The residue thereby obtained was purified via column chromatography on silica gel by eluting with 1:3 EtOAc-ligroin. Pure 3 (2.65 g, 80 percent) was thereby obtained as a pale yellow oil: bp 72-74 °C (0.4 mm Hg) [lit.(Reference 13) bp 50-52 °C (0.1 mm Hg)]; IR (See Table A-1); ^1H NMR ($CDCl_3$) δ 0.98 (s,9 H), 3.66 (m,4 H), 4.99 (m,1 H); ^{13}C NMR ($CDCl_3$) δ 24.67 (q), 51.60 (t), 52.43 (s), 71.57 (s).

c. *N-t*-Butyl-3-nitro-3-(*N'-t*-butyl-3'-nitroazetidin-3'-yl)azetidine (4)

To a solution of KO*t*-Bu (2.55 g, 22.8 mmol) in EtOH (100 mL) under nitrogen was added a solution of **3** (3.00 g, 19.0 mmol) in EtOH (5 mL), and the resulting mixture was allowed to stir at room temperature for 3 h. Compound **2** (4.50 g, 19.0 mmol) then was added, and the resulting mixture was allowed to stir at ambient temperature for 48 h. The reaction mixture was concentrated *in vacuo*. Water (60 mL) was added to the residue, and the resulting aqueous suspension was extracted with CH_2Cl_2 (3 x 40 mL). The organic layer was washed with water (2 x 50 mL), dried (Na_2SO_4), and filtered, and the filtrate was concentrated *in vacuo*.

To a solution of the residue thereby obtained (6.0 g) in EtOH (80 mL) at room temperature under nitrogen was added dropwise a solution of $NaBH_4$ (1.20 g, 31.7 mmol) in 60 percent aqueous EtOH (40 mL), and the resulting mixture was stirred at room temperature for 5 h. The reaction mixture then was concentrated *in vacuo*. Water (60 mL) was added to the residue, and the resulting aqueous suspension was extracted with CH_2Cl_2 (3 x 40 mL). The organic layer was washed with water (2 x 25 mL), dried (Na_2SO_4), and filtered, and the filtrate was concentrated *in vacuo*. The residue thereby obtained was purified via column chromatography on silica gel by eluting with 1:5 EtOAc-ligroin. This procedure afforded pure **4** (1.16 g, 19 percent) as a slightly yellowish microcrystalline solid: mp 117-118 °C; IR (See Table A-1); ^{1}H NMR ($CDCl_3$) δ 1.05 (s, 9 H), 3.9 (AB, J_{AB} = 9.0 Hz, 2 H); ^{13}C NMR ($CDCl_3$) δ 24.57 (q), 52.76 (s), 54.18 (t), 83.71 (s). Anal. Calcd for $C_{14}H_{26}N_4O_4$: C, 53.49; H, 8.34. Found: C, 53.60; H, 8.24. The structure of **4** was established unequivocally via application of X-ray crystallographic techniques *(vide infra)*.

Continued elution of the chromatography column afforded a second fraction which contained recovered **4** (2.5 g, 83 percent). The IR, ^{1}H NMR, and ^{13}C NMR spectra of the compound thereby obtained were identical in all respects with the corresponding spectra of authentic **4** (Reference 13) *(vide supra)*.

d. 1,3-Dinitro-3-(1',3'-dinitroazetidin-3'-yl)azetidine (TNDAZ)

A solution of **4** (1.17 g, 3.73 mmol) in fuming HNO_3 (40 mL) was prepared, and the resulting solution was refluxed for 40 h. *[CAUTION.- When preparing a solution of 4 in fuming HNO₃, care should be taken to add the solid dimer in small portions with stirring to fuming nitric acid. Inverse addition of reagents may result in fire and/or explosion.]* The reaction mixture was allowed to cool gradually to ambient temperature and then was poured slowly with stirring into ice-water (60 mL), whereupon a colorless precipitate was formed. The precipitate was collected by suction filtration and was washed with cold water until the washings became neutral to litmus (150 mL). The resulting solid material was air-dried, thereby affording **TNDAZ** (830 mg, 77 percent)

as a colorless microcrystalline solid: mp 171-173 °C (dec.). Analytically pure **TNDAZ** was obtained by recrystallizing this material from EtOAc-ligroin as colorless platelets: mp 171-172 °C (dec.); IR (See Table A-1); ^{1}H NMR (CDCl$_3$) δ 4.8 (AB, J_{AB} = 15.0 Hz, 2 H), 5.05 (AB, J_{AB} = 15.0 Hz, 2 H); ^{13}C NMR (CDCl$_3$) δ 62.73 (t), 80.44 (s). Anal. Calcd for C$_6$H$_8$N$_6$O$_8$: C, 24.67; H, 2.76. Found: C, 24.80; H, 2.63.

2. STRUCTURAL CHARACTERIZATION

Pertinent details regarding the X-ray characterization of **TNDAZ** are presented in Table 1.

Table 1. X-ray structure data for **TNDAZ** and **4**.

	TNDAZ	**4**
Formula	C$_{14}$H$_{26}$N$_4$O$_4$	C$_6$H$_8$N$_6$O$_8$
Size (mm)	0.31 x 0.35 x 0.42	0.04 x 0.21 x 0.23
Space Group	C2/c	P2$_1$/c
a (Å)	17.092 (1)	15.154 (2)
b (Å)	10.8654 (6)	11.513 (1)
c (Å)	10.640 (1)	12.903 (1)
α (°)	90	90
β (°)	120.910 (7)	93.316 (9)
γ (°)	90	90
V (Å^3)	1695.3 (3)	2247.4 (4)
Z	4	8
D$_c$ (g-cm^{-3})	1.232	1.727
μ (cm^{-1})	1.23	1.51
(2θ$_{max}$)	50	40
Total refl.	1618	2338
Unique refl.	1571	2241
R$_{int}$	0.035	0.031
I ≥ 3σ(I)	1040	616
Parameters	100	161
R, wR	0.0527, 0.0479	0.0597, 0.0627
(Δ/σ)$_{max}$	<0.01	<0.01
ρ$_{min}$;ρ$_{max}$	0.19, -0.18	0.29, -0.26

The X-ray crystal structure shows the solvent-recrystallized molecule to be oriented in a "boat" configuration with respect to the two rings (Figure 1).

7

3. THERMAL CHARACTERIZATION

a. Thermal Properties of Neat **TNDAZ**

Individual crystals of solvent-recrystallized **TNDAZ**, heated at 5 °C/m in the hot stage microscope, underwent an apparent solid-solid transition at 170.8 °C, just prior to melting at 171.2-171.5 °C. The melting range for a large sample of crystals is 170.1-172.3 °C with no solid-solid transition apparent prior to melting, presumably due to the opaqueness of the sample. The pre- and post-transition polymorphs are hereinafter designated **TNDAZ (I)** and **TNDAZ(II)**, respectively.

Thin crystalline films of **TNDAZ,** applied to a microscope slide with coverplate and crystallized from the melt by both crash-cooling (~140 °C/m) and programmed cooling (5 °C/m), exhibit a dendritic structure characterized by multi-polarization colors generally emanating from a point source. While the crystal habit of a **TNDAZ** thin film does not appear to be influenced greatly by the cooling process, the affect on shrinkage crack size and pattern is significant. Specifically, **TNDAZ** that has been crash-cooled is characterized by macro-shrinkage cracks forming irregularly-shaped sections, within which are micro-shrinkage cracks in a concentric ring pattern and in random locations (Figure 2). A **TNDAZ** thin film, program-cooled, is characterized by micro-shrinkage cracks located perpendicular to the dendritic structure and generally showing evidence of limited thermal decomposition by the presence of many gas bubble remnants (Figure 3).

Programmed heating (5 °C/m) of a crash-cooled **TNDAZ** thin film resulted in a significant polarization color pattern change in the 110-115 °C temperature range and a general darkening of the film, but did not affect the shrinkage crack pattern (Figure 4). This change is believed to result from an annealing process that relieves lattice strain induced by the cooling process. Continued heating of this same **TNDAZ** thin film produced still another polarization color change at 158.5 °C that is believed to be associated with the solid-solid (polymorph) transition from **TNDAZ (I)** to **TNDAZ(II)**. Subsequent experiments with thin crystalline films showed this transition always occurred in the temperature range 151-162 °C. The color change, shown in Figure 5, occurred as paintbrush-like strokes of purple moving from left to right across the lower four-fifths of the field of view, then in an upward direction as a linear front until the entire sample was purple. The basic underlying structure of shrinkage cracks remained unchanged. Subsequent cooling to 138.7 °C resulted only in a lightening of the purple color. Continued heating at 5 °C/m resulted in melting in the temperature range 171.2 - 171.5 °C. Upon crash-cooling and reheating at the same rate, the solid-solid transition occurred at 160.1 °C.

8

A thin crystalline film of **TNDAZ (I)**$_{Strained}$, heated at 5 °C/m through the 150-160 °C temperature range without a hold, resulted in melting temperature ranges for both **TNDAZ (I)** and **TNDAZ(II)** at 170.1-171.6 and 171.3-172.2 °C, respectively. At the initiation of melting for the former, the solid-solid transition had progressed only about one-fourth the way across the visible sample surface. The combination of these two temperature ranges, should the solid-solid transition not be observable such as with a large sample of HSM-opaque crystals or with a DSC operation, is 170.1-172.2 °C.

DSC melting operations, carried out with both solvent-recrystallized (a) and crash-cooled (b) **TNDAZ (I)**, and with **TNDAZ (II)** (c) yielded melting temperature ranges (onset/peak) of (a) 170.9/172.1, (b) 172.0/173.4 and (c) 172.1/173.0 °C. The range for (a) is consistent with that from the HSM operation with (a), while being distinctly different from that of (b) and (c). The similarity of the latter two values suggests that the solid-solid transition from **TNDAZ (I)** to **(II)** was completed prior to melting. The heat of fusion for (a) was 6.099 Kcal/mol. Upon programmed cooling (DSC) of **TNDAZ** from the liquid state, an exothermic, unresolved doublet was observed at 122-124 °C. **TNDAZ** exothermically decomposed at 241/256 °C (onset/peak) with an associated energy of 187 Kcal/mol.

Three HSM cooling operations, carried out at 5 °C/m with **TNDAZ**$_{(I)}$, yielded crystallizations at 131.9, 127.8 and 150.1 °C. The first two were followed by solid-solid transitions at 129.5 and 127.6 °C, respectively, while the latter yielded only a single event. The cooling doublet observed during DSC cooling operations is consistent with this double crystallization finding. The crystallization fronts associated with the liquid-solid transitions for the first two events were continuous and irregular (Figure 6), while that for the latter resembled flattened rods (Figure 7). Upon heating the final product from these cooling operations, none of the thin films underwent any significant surface texture change or darkening prior to melting in the temperature range 170.7-172.6 °C.

These HSM cooling experiments were followed by two at rates of approximately 70 °C/m that yielded single event crystallizations at 109 and 102.4 °C. The crystallization fronts were continuous and irregular, similar to those observed from the first two events described in the previous paragraph. Both of these thin films, when heated to melting, underwent significant surface texture roughening with associated darkening over the temperature range 155-170 °C prior to melting at 171.0-171.8 (5 °C/m). In addition, a small area of the thin film that crystallized at 109 °C underwent a change at 111.6 °C, which is within the temperature range for the annealing process associated with the change from **TNDAZ (I)**$_{strained}$ to **TNDAZ (I)**$_{annealed}$. While the surface texture roughening/darkening may be associated with the solid-solid transition to **TNDAZ (II)**, the primary component of these two thin crystalline films is believed to be **TNDAZ (I)**$_{annealed}$. Based on the melting points, the lack of surface texture change

9

prior to melting and the shape of the crystallization fronts from the liquid state, the final thin films from the three cooling operations described in the previous paragraph are believed to be **TNDAZ (II)**, with the lower temperature events initially yielding **TNDAZ (I)**.

b. Thermal Characterization of **TNAZ**

Thin crystalline films of **TNAZ** were melted (99.0-100.7 °C), held at 109 °C for at least two minutes, then cooled at rates of 5 and of approximately 30 °C/m. During the heating process the thin film darkened significantly. All liquids underwent spontaneous double crystallizations in the temperature range 46-61 °C. The structure of the initial crystallization product is dendritic with a loosely compacted appearance, while that of the second crystallization product, also dendritic, was of a very compact appearance with characteristic macro-shrinkage cracks. The latter are formed spontaneously behind the second crystal front as it progresses across the initial solid (Figure 8). This recrystallization characteristic, apparent compactness with associated, spontaneously-formed macro-shrinkage cracks, suggests the density of the stable crystalline film is greater than that of the initial, unstable crystalline film. The stable polymorph is hereinafter designated **TNAZ (I)** and the unstable **TNAZ (II)**.

DSC operations at a heating rate of 5 °C/m with solvent-recrystallized **TNAZ** afforded a sharp melting event at 99.3/101.1 °C (onset/peak) with an associated heat of fusion of 6.405 Kcal/mol and with no evidence of thermal degradation. Upon programmed cooling, liquid **TNAZ** exhibited only an exothermic singlet at 54-55 °C. **TNAZ** exothermically decomposed at 244/256 °C (onset/peak) with an associated energy of 107 Kcal/mol.

c. Analysis by High Performance Liquid Chromatography

Prior to thermal analysis operations, both **TNDAZ** and **TNAZ** were subjected to analysis by high performance liquid chromatography (HPLC). Their purities, determined by the area normalization method, were 98.2 and 97.8 percent, respectively.

d. Phase Diagram

The eutectic composition and melting temperature for the two component system, **TNDAZ/TNAZ**, was calculated using a computer program in GW Basic. The program iteratively solves equation 1 using heats of fusion and melting points from both components as input data,

$$Rlnx = \Delta H_{fus} (-1/T + 1/T_o) \qquad (1)$$

where T is the melting point (°K) of the eutectic composition and T_o, ΔH_{fus} and x are the

10

melting point, heat of fusion and mole fraction of component A or B, respectively, and R is the gas constant (1.987). The calculated melting point and mol percentage value for the **TNAZ** component in the eutectic composition are 90.9 °C and 78.5, respectively. While the GW Basic program provides a graphical presentation of the phase diagram, a corresponding list of associated temperatures for the melting of each component into the eutectic composition is not provided. These temperatures were obtained by solving equation 1 for each component at selected mol fraction values.

e. DSC Characterization of **TNAZ/TNDAZ** mixtures

The first heating operations for twenty-one, freshly ground **TNAZ/TNDAZ** mixtures afforded a consistent, endothermic event at an average temperature of 90.7 ± 0.1 °C that is caused by eutectic melting. The mixtures containing greater than 78.5 mol percent **TNAZ** also yielded a second endothermic event that is attributed to the dissolution of the **TNAZ** component into the liquid eutectic composition.

Remeasurements of these endothermic events with samples obtained by freezing of the initial melts resulted in a shift of the eutectic endothermic events to an average temperature of 87.5 ± 0.1 °C. The eutectic melting points from the initial and subsequent remelting operations are hereinafter referred to as "eutectic (1)" and "eutectic (2)", respectively. Remelting operations, carried out after time delays at room temperature ranging from 8 to 20 days, showed that eutectic (2) had partially reverted to eutectic (1). The melting points from all of these DSC operations are compiled in Table 2. A composite plot of the DSC thermograms from first, second and third melting operations with a **TNAZ/TNDAZ** mixture containing 96.7 mol percent **TNAZ** is shown in Figure 9.

Crystallization temperatures and heats of crystallization associated with these mixtures were inconsistent throughout this study, presumably resulting from extensive supercooling processes. As a result, only the melting temperatures and heats of fusion associated with the mixtures are reported. The heats of fusion for all of the mixtures are shown in Table 3.

f. HSM Characterization of **TNAZ/TNDAZ** Mixtures

A mixed fusion slide was prepared according to the method described in McCrone (Reference 14). After the higher melting component (**TNDAZ**) was melted onto the slide with coverplate, the lower melting component (**TNAZ**) was then melted and allowed to wick under the coverplate until it contacted the solid **TNDAZ**. The edges of the coverplate in contact with the zone of mixing were then sealed with an epoxy cement to prevent encroachment of air into the eutectic melt during the cooling process, a detrimental characteristic that may ruin the slide before recrystallization occurs. The

11

slide was program-heated from 59.5 °C at 1 °C/m until melting occurred in the zone of mixing over the temperature range 88.0-91.4 °C, eutectics (1) and (2). As seen with the individual components, the polarization color patterns associated with **TNDAZ** changed significantly during this heating process, while that of **TNAZ** only darkened followed by lightening during the melting of the eutectic zone. Gas bubbles observed in the melt zone are believed to have resulted from air trapped at the **TNAZ/TNDAZ** interface during the slide preparation. A reheating operation at 1 °C/m resulted in remelting of the zone of mixing at 87.8-88.9 °C (eutectic 2). The resolidified zone of melting, after being crash-cooled rapidly, is characterized by finely granulated eutectic composition (Figure 10). The **TNAZ** is characterized by macro-shrinkage cracks away from the eutectic zone and overlaying flattened rods of **TNDAZ** that migrated across the zone of mixing during the melting operation.

HSM heating operations with ten intimately ground mixtures of **TNAZ/TNDAZ** afforded melting points for the eutectic (1) and eutectic (2) compositions (average values of 90.8 and 87.9 °C, respectively) and for **TNAZ** that were consistent with those from both DSC operations and calculations. These data are summarized in Table 4. Melting points for the **TNDAZ** component were not observed during DSC operations, but were obtained for two mixtures rich in **TNDAZ** by HSM operations. The dissolution of **TNDAZ** in the eutectic (1 and 2) melt is slow and requires remelting operations to affect melting of the original crystals. As a result, the data are inconsistent. The characteristics of the residual crystals after the melting of eutectic (1) for mixtures around the calculated eutectic composition suggest that the **TNAZ** component lies between the mol percent values of 78.8 and 78.0, which is consistent with the calculated value of 78.5. The calculated phase diagram, along with all of the DSC- and HSM-generated data, is shown in Figure 11. The unassigned data could not be unequivocally related to any particular melting event, even from HSM observations.

After initial melting operations with freshly ground **TNAZ/TNDAZ** mixtures followed by crash-cooling, the typically light-colored, textured surface rapidly developed randomly patterned blackish areas upon reheating (Figure 12a). Continued heating resulted in the overall surface darkening and becoming more textured in appearance (Figure 12b and c). The general appearance of the surface of any of the **TNAZ/TNDAZ** mixtures suggests the volume of the sample has increased vertically, the dark areas resulting from a dimming of the underlighting as it passes through the roughened, upward projecting, angular surface.

g. Modified Vacuum Thermal Stability Tests

     Pure **TNDAZ**, **TNAZ** and a **TNDAZ/TNAZ** mixture containing 77 mol percent **TNAZ** were subjected to thermal stability testing using the MVTS technique. The results are shown in Table 5.

Table 2. Endothermic Peak Temperatures for Selected DSC Melting Operations with
TNDAZ/TNAZ Mixtures

	Melting Points (°C)				Time-Delayed Remelt (°C)	
Mol Percent **TNAZ**	Eutectic(1)	**TNAZ**	Eutectic(2)	**NA**[1]	Eutectic	(Days)
96.7	90.4	98.5	87.4		86.5	(20)
93.3	90.5	98.3	87.4			
90.0	90.5	95.1	86.9			
85.9	91.0	94.3	88.1		88.0/90.7	(13)
85.0	90.8	93.1	87.2	92.4	90.3	(20)
84.0	90.6	93.5	87.2	91.8		
83.0	90.7	92.3	87.5	91.9	86.8/89.4	(20)
82.0	91.2	93.0	87.8	91.2		
81.0	91.2		87.7	90.4		
80.0	90.6	92.0	87.5	90.2	87.4/90.8	(8)
79.5	90.5	91.5	87.6	89.9		
78.8	90.6	90.6	87.2	89.7	87.2/90.7	(8)
78.5	90.6		87.0	90.2		
78.0	90.9		87.5	89.1		
77.0	90.8		87.8	89.7		
75.3	91.4		87.5	89.5		
73.8	90.5		87.2	89.3	86.5/89.4	(13)
70.0	90.9		87.4	89.7		
60.3	91.0		87.7			
50.0	90.6		N.D.[2]			
30.0	89.8		N.D.[2]			
Average	90.7		87.5			

1. Unassigned.
2. Not determined.

Table 3. Heats of Fusion from First Melting Operations[1]

| TNAZ | | Heats Of Fusion (Cal/Gm) | | |
Mol Percent	Wt Percent	Theory	Measured	Eut./Gm
100	100		33.33	
96.7	95.1	32.72[2]	32.00	25.27[3]
93.3	90.2	32.12[2]	30.57	25.04[3]
90.0	85.5	31.52[2]	29.28	25.13[3]
85.9	80.0	30.83[2]	27.87	25.30[3]
85.0	78.8	30.68[2]	28.37	26.45[3]
84.0	77.5	30.52[2]	28.29	26.74[3]
83.0	76.2	30.36[2]	28.17	26.96[3]
82.0	75.0	30.23[2]	27.28	26.21[3]
81.0	73.7	30.05[2]	26.42	25.61[3]
80.0	72.5	29.91[2]	27.22	26.80[3]
79.5	71.8	29.81[2]	28.04	27.81[3]
78.8	71.0	29.73[2]	27.08	26.99[3]
78.5	70.6	29.67[2]	27.02	27.02
78.0	70.0	29.43[4]	26.00	26.21[5]
77.0	68.8	28.93[4]	26.45	27.13[5]
75.3	66.7	28.04[4]	24.24	25.65[5]
73.8	64.8	27.32[4]	23.85	25.87[5]
70.0	60.5	25.42[4]	23.26	27.14[5]
60.3	50.0	21.01[4]	18.62	26.30[5]
50.0	39.7	16.68[4]	14.97	26.64[5]
30.0	22.0	9.25[4]	8.33	26.70[5]
0.00			20.89	

1. DSC.
2. (33.33)(wt fraction **TNAZ**) + (20.89)(wt fraction **TNDAZ**).
3. [Measured value - [(33.33)(wt fraction excess **TNAZ**)]]/wt fraction eutectic.
4. [(33.33)(wt fraction **TNAZ**) + (20.89)(wt fraction **TNDAZ**)] - (20.89)(wt fraction excess **TNDAZ**).
5. Measured value/wt fraction eutectic.

Table 4 Melting Points from Hot Stage Microscope Operations with Selected
    TNAZ/TNDAZ Mixtures[1]

Mol Percent	Melting Points (°C)					
TNAZ	**TNAZ**	Eutectic(1)	Eutectic(2)	**TNDAZ**	Unassigned	Comments
96.7	98.7	91.2	88.2			2
90.0	96.6	91.2	88.1			2
85.9	94.6	91.2	88.0			2
82.0	93.2	90.7	88.0			2
80.0	91.4	90.1	88.6			2
78.8	91.6	91.3	87.6		88.4	2, 3
78.5		>89.1	88.2		94.5	2
78.0		90.8	87.3			2, 4
77.0		90.6	87.5	93.0-94.0	89.8	2
75.3		90.5	87.7	97.5, 95.1, 94.7, 93.2		2
Average		90.8	87.9			

1. Samples heated at 1 °C/m.
2. After the initial melting operation the samples were rapidly cooled and reinserted into the hot stage at various temperatures (60, 68, 69 and 84 °C). The surface characteristics of the samples rapidly changed from a yellow-green, grainy appearance to one with significant darkened (blackish) areas. Closer inspection suggested that the sample volume increased vertically and that at least some of the dark-appearing areas were caused by a dimming of the underlighting as it passed through a roughened angular surface.
3. Final crystals to melt were needles similar to that observed with pure **TNAZ**.
4. Final grain-like crystals remaining were similar to those observed with pure **TNDAZ**, temperature not increased beyond 92 °C.

Table 5. Modified Vacuum Thermal Stability Test Results

|	TNDAZ[1]	TNAZ[2]	Mixture[1]
Pressure (mm)	47.31	45.90	40.71
Mols Gas	4.57e-5	4.40e-5	3.92e-5
Total Volume Gas @ STP (cm^3)	1.02	0.99	0.88
Sample Weight (mg)	100.1	501.0	108.1
Volume Gas Components (cm^3)			
$\quad N_2$	0.07	0.03	0.06
$\quad CO$	0.01	-----	0.003
$\quad NO$	0.03	0.01	0.05
$\quad CO_2$	0.09	0.01	0.04
$\quad N_2O$	0.02	0.004	0.01
$\quad H_2O$	0.85[3]	0.49[4]	0.52[3]
$\quad$ Other	----	0.44 (EtOH)	0.04 (EtOH)
$\quad$ Total Gas	1.07	0.99	0.71
$\quad$ Total - (H_2O, EtOH)	0.22[5]	0.065[5]	0.16[5]

1. Data obtained from a single sample.
2. Data obtained in triplicate.
3. Water volume obtained by gas chromatographic analysis.
4. Water volume obtained by difference [total volume - (decomposition gases + EtOH)].
5. Not normalized to unit weight.
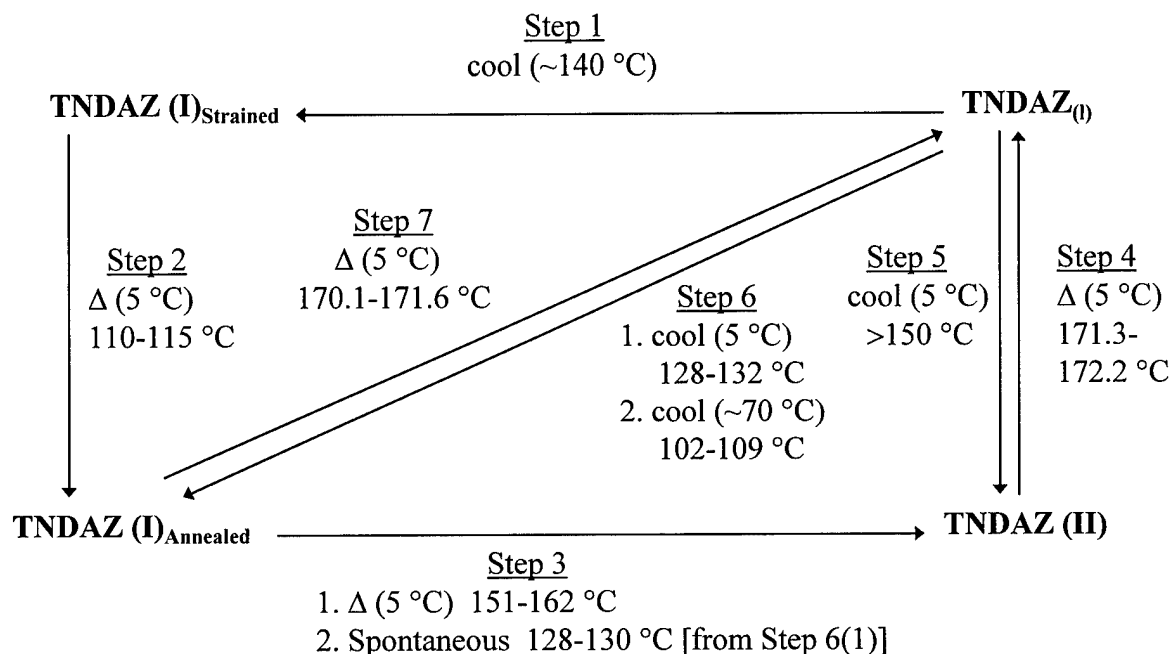
SECTION IV

DISCUSSION

The synthesis of **TNDAZ** is shown in Scheme 1. The starting material for this reaction sequence, i.e., **1**, was prepared by using the method reported by Hiskey and Coburn (Reference 4). Treatment of **1** with a solution of Br_2 in aqueous base resulted in retro-Henry reaction (Reference 15) with concomitant bromination of the resulting nitro-stabilized anion, thereby producing **2**. Subsequent reaction of **2** with $NaBH_4$-EtOH resulted in selective reduction of the carbon-bromine bond in **2**, thereby affording **3** in good yield. Subsequent reaction of **3** with KOt-Bu-EtOH resulted in formation of the corresponding α-nitro carbanion which then was reacted with **2** to form a mixture of the corresponding 3'-azetidinyl-3-azetidine (**4**) along with unreacted **2**. In our hands, this mixture of **4** and **2** could not be separated, either by fractional recrystallization or by column chromatography. It proved advantageous to react this mixture as obtained with $NaBH_4$. Under these conditions, **2** is reduced to **1**, but **4** remains unaffected. The resulting mixture of **4** and **1** can be separated readily via column chromatography. The structure of **4** was established unequivocally via application of X-ray crystallographic methods. Finally, when refluxed with fuming nitric acid, **4** was converted into the target molecule, **TNDAZ**, in good yield.

Scheme 1

18
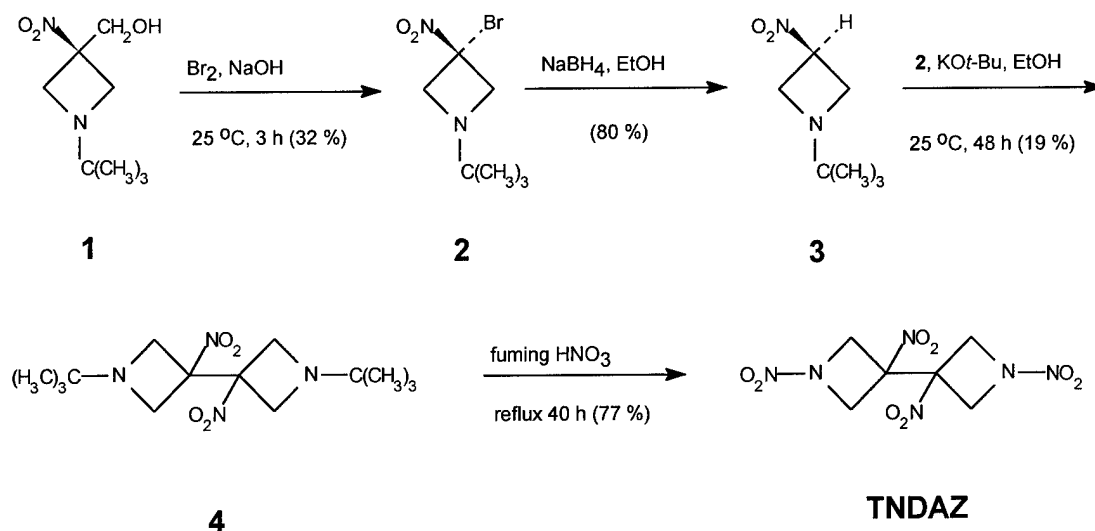
It has been demonstrated from both heating and cooling operations that **TNDAZ** exists in at least two polymorphic forms, **(I)** and **(II)**. The sequence of conditions used to obtain these polymorphs is shown in Scheme 2.

Scheme 2

Step 1
cool (~140 °C)

TNDAZ (I)$_{Strained}$ ←─────────────────────── **TNDAZ**$_{(I)}$

Step 7
Δ (5 °C)

Step 2   170.1-171.6 °C   Step 5   Step 4
Δ (5 °C)   Step 6   cool (5 °C)   Δ (5 °C)
110-115 °C   1. cool (5 °C)   >150 °C   171.3-
                                          128-132 °C   172.2 °C
                                      2. cool (~70 °C)
                                          102-109 °C

TNDAZ (I)$_{Annealed}$ ─────────────────────────→ **TNDAZ (II)**

Step 3
1. Δ (5 °C) 151-162 °C
2. Spontaneous 128-130 °C [from Step 6(1)]

The thin crystalline films of both polymorphs of **TNDAZ** are characterized by a dendritic structure with associated shrinkage cracks, the size (micro vs macro) and orientation of which are dependent on the rate of cooling. The shrinkage cracks generally form below 50 °C. Both polymorphs are stable at ambient temperature, (II) for at least 15 days. FTIR spectra (KBr) in the region 4000-500 cm^{-1}, obtained from the solid **TNDAZ** species shown in Scheme 2 and from solvent-recrystallized **TNDAZ**, are similar (Figure 13).

Similarly, **TNAZ** exhibits at least two polymorphic forms, **(I)** and **(II)**. The unstable polymorph, **(II)**, is observed only during the crystallization process from liquid **TNAZ**. It spontaneously transitions to the stable form, **(II)**, at ≥ 30 °C, while simultaneously forming macro-shrinkage cracks. The change in appearance of the thin film during the transition from **(II)** to **(I)**, loosely packed to compact dendritic with macro-shrinkage cracks, is consistent with a density increase and offers a logical explanation for the undesirable (highly porous) castings obtained with neat **TNAZ**.

It was also demonstrated that binary mixtures of **TNDAZ** and **TNAZ** result in a eutectic mixture that is influenced by polymorphism. Eutectic (1), formed from the initial melting of the dry powder mixture, transitions to eutectic (2) during remelting

19

operations. The latter exhibited limited stability at ambient temperature before transitioning back to (1). The experimental melting point data for the mixtures, obtained by both DSC and HSM operations, was consistent with the binary phase diagram (eutectic (1) only) calculated using DSC-generated melting temperatures and heats of fusion for the individual solvent-recrystallized components.

The explosives community subjects all developmental energetic materials and formulations to a series of small scale safety tests prior to any scale-up operations. This test series is directed at determining thermal sensitivity and includes dynamic and isothermal DSC experiments and time-to-explosion and vacuum thermal stability tests. In accordance with this general operating procedure, **TNDAZ, TNAZ** and a 77:23 **TNAZ-TNDAZ** binary mixture were subjected to the MVTS test. The data derived from these tests show that **TNAZ** exhibits excellent thermal stability relative to the test conditions, whereas **TNDAZ** evolves an unacceptable quantity of gas associated with thermal decomposition. This finding renders **TNDAZ** unacceptable for scale-up operations. While the MVTS data suggest the two components of the mixture are compatible, the mixture itself evolves a near unacceptable quantity of gas, therefore, is only marginally acceptable for scale-up operations. This gas generation from the mixture is presumably due to the lower thermal stability of the **TNDAZ** component. The standard used commonly throughout the explosives community states that any material which evolves 2.0 cm^3/g of gas during the MVTS test is deemed unacceptable for further operations. The total gas volumes shown in Table 5 for each component and the mixture, when normalized to one gram of sample, are 22.0, 0.13 and 14.8 cm^3/g, respectively.

SECTION V

CONCLUSIONS

TNDAZ was prepared via a 4-step synthesis route, and its structure was established unequivocally via application of single-crystal X-ray crystallographic methods. This compound was thermally characterized by using both DSC and HSM techniques, and it was found to undergo limited decomposition at its melting point.

The results of a DSC study provided melting point and heat of fusion data for **TNDAZ**. Analysis of crystalline films using a hot stage microscope for both heating and cooling operations provided evidence that **TNDAZ** exists in at least two polymorphic forms, **(I)** and **(II)**.

Analysis of thin crystalline films of **TNAZ** by HSM cooling operations afforded evidence, in the form of double crystallizations, of polymorphism. At least two polymorphs of **TNAZ** were observed, **TNAZ (I)** (stable at ambient temperature) and **TNAZ (II)** (unstable).

Polymorphism was also exhibited by the binary mixtures of **TNAZ** and **TNDAZ**. The melting point of the initial eutectic (1) composition, obtained from the heating operation on freshly ground mixtures, decreased by 4 °C for re-melting operations, eutectic (2). It was later shown that eutectic (2) slowly reverts to eutectic (1) at ambient temperature. The phase diagram for the **TNAZ-TNDAZ** binary system was calculated for eutectic (1), and was confirmed experimentally by DSC and HSM melting operations.

Data from modified vacuum thermal stability tests with both **TNDAZ** and a 77:23 **TNAZ-TNDAZ** binary mixture indicate that (i) **TNDAZ** is unacceptable for scale-up operations and (ii) the binary mixture is only marginally acceptable. This conclusion was based on a standard used commonly throughout the explosives community: i.e., any material which evolves 2.0 cm^3/g of gas during the MVTS test is deemed unacceptable.

21

REFERENCES

1. Archibald, T. G.; Gilardi, R.; Baum, K.; George, C. *J.* Org. Chem. *1990*, 55, 2920.

2. (a) Axenrod, T.; Watnick, C.; Yazdehkasti, H.; Dave, P. R. *Tetrahedron Lett.* **1993**, 34, 6677. (b) Axenrod, T.; Watnick, C.; Yazdehkasti, H.; Dave, P. R. *J. Org. Chem.* **1995**, 60, 1959.

3. Katritzky, A. R.; Cundy, D. J.; Chen, J. *J. Heterocyclic Chem.* **1994**, 31, 27 1.

4. Hiskey, M. A.; Coburn, M. D. U. S. Patent 5,336,784; *Chem. Abstr.* **1994**, 121, 300750s.

5. Marchand, A. P.; Rajagopal, D.; Bott, S. G.; Archibald, T. G. *J. Org. Chem* **1995**, 60, 4943.

6. Ongoing work at the Armament Directorate, Energetic Materials Branch, Eglin AFB, Florida.

7. (a) Aubert, S. A., McKenney, R. L., Jr., Sprague, C. T., Characterization of a TNAZ/PETN Composite Explosive, WL-TR-96-7012, Wright Laboratory/Armament Directorate, Eglin AFB, Florida, 30 April 1996. (b) Aubert, S. A., Sprague, C. T., Characterization of a TNAZ/TNB Composite Explosive, WL-TR-96-7013, Wright Laboratory/Armament Directorate, Eglin AFB, Florida, 30 May 1996.

8. (a) The authors have deposited atomic coordinates for these structures with the Cambridge Crystallographic Data Center. They can be obtained, on request, from the Director, Cambridge Crystallographic Data Center, 12 Union Road, Cambridge CB2 1EZ, UK. (b) Mason, M. R.; Smith, J. M.; Bott, S. G.; Barron, A. R. *J. Am. Chem. Soc.* **1993**, 115, 4971.

9. Main, P.; Fiske, S. J.; Hull, S. E.; Lessinger, L.; Germain, G.; DeClerq, J. P.; Woolfson, M. *M. MULTAN80, A System of Computer Programs for the Automatic Solution of Crystal Structures from X-ray Diffraction Data,* University of York: England; 1980.

10. *MolEN, An Interactive Structure Solution Program;* Enraf-Nonius: Delft, The Netherlands; 1990.

11. Cromer, D. T.; Waber, J. T. *International Tables for X-ray Crystallography;* Kynoch Press: Birmingham; Vol. IV, 1974, Table 2.

12. (a) Benchabane, M., *J. Energetic Materials,* **1993**, 11 (2), 89-100. (b) A Wright Laboratory technical report describing the MVTS system is currently being drafted.

13. Visiting Scientist, on sabbatical leave from Indian Institute of Chemical Technology, Hyderabad, A. P. India.

14. McCrone, W. C. ,Jr., <u>Fusion Methods in Chemical Microscopy</u>, 94-101, Interscience Publishers, Inc., NY, 1957.

15. For a review of the Henry reaction, see: Baer, H. H.; Urbas, L. In: Feuer, H. (ed.) "TheChemistry of the Nitro and Nitroso Groups", Wiley-Interscience: New York, 1970, Part 2, pp 76-117.

16. Personal communication with Dr. Howard H. Cady, Los Alamos National Laboratory, Los Alamos, N. M.
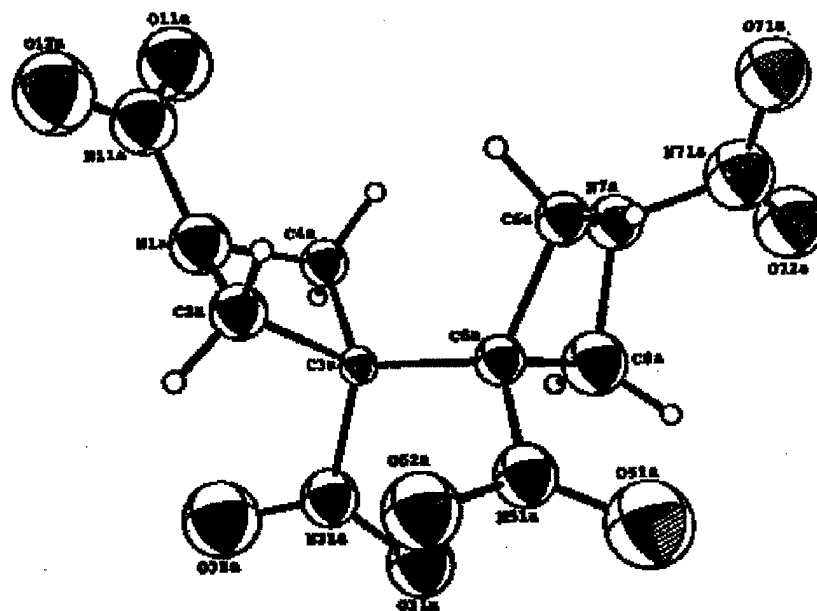
Figure 1. X-ray crystal structure of **TNDAZ (I)**

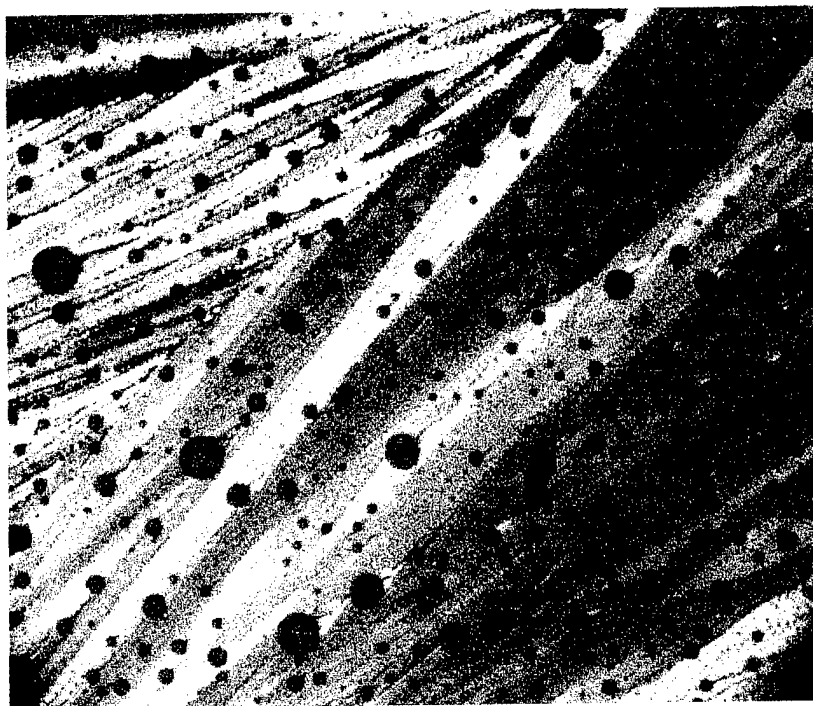Figure 2. Characteristic thin crystalline film of crash-cooled **TNDAZ (I)**_{Strained}

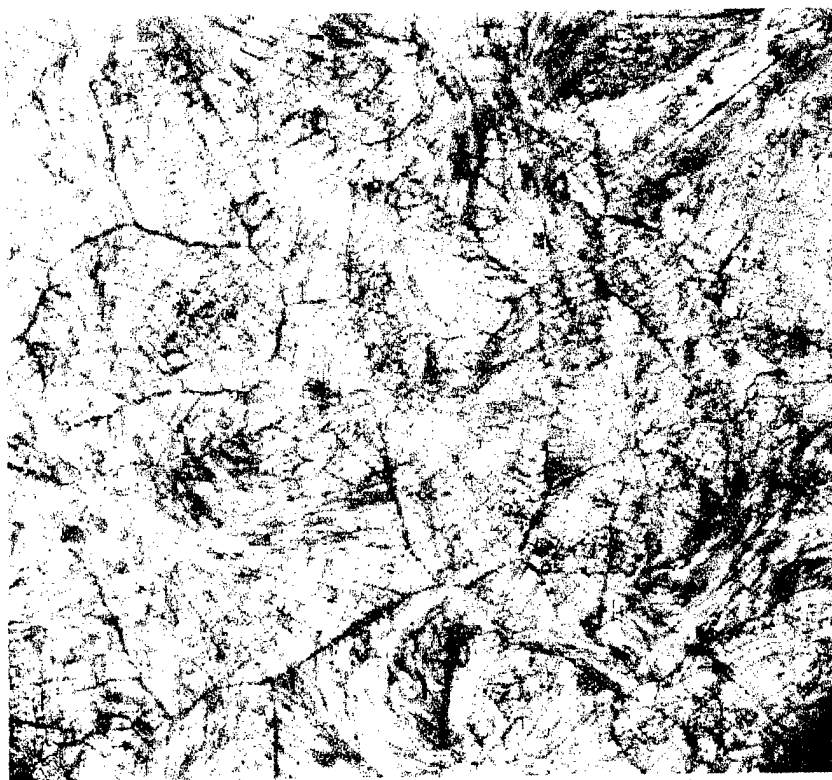Figure 3. Characteristic thin crystalline film of program-cooled (5 °C) **TNDAZ** (I)$_{Annealed}$

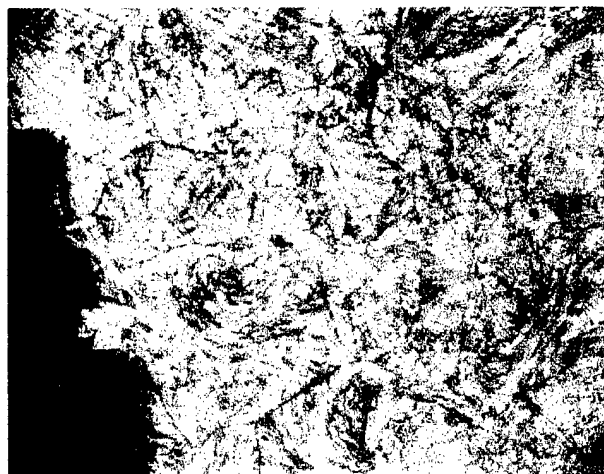Figure 4. Thin crystalline film of **TNDAZ** (I)$_{Annealed}$ obtained by heating **TNDAZ** (I)$_{Strained}$ to 110-115 °C

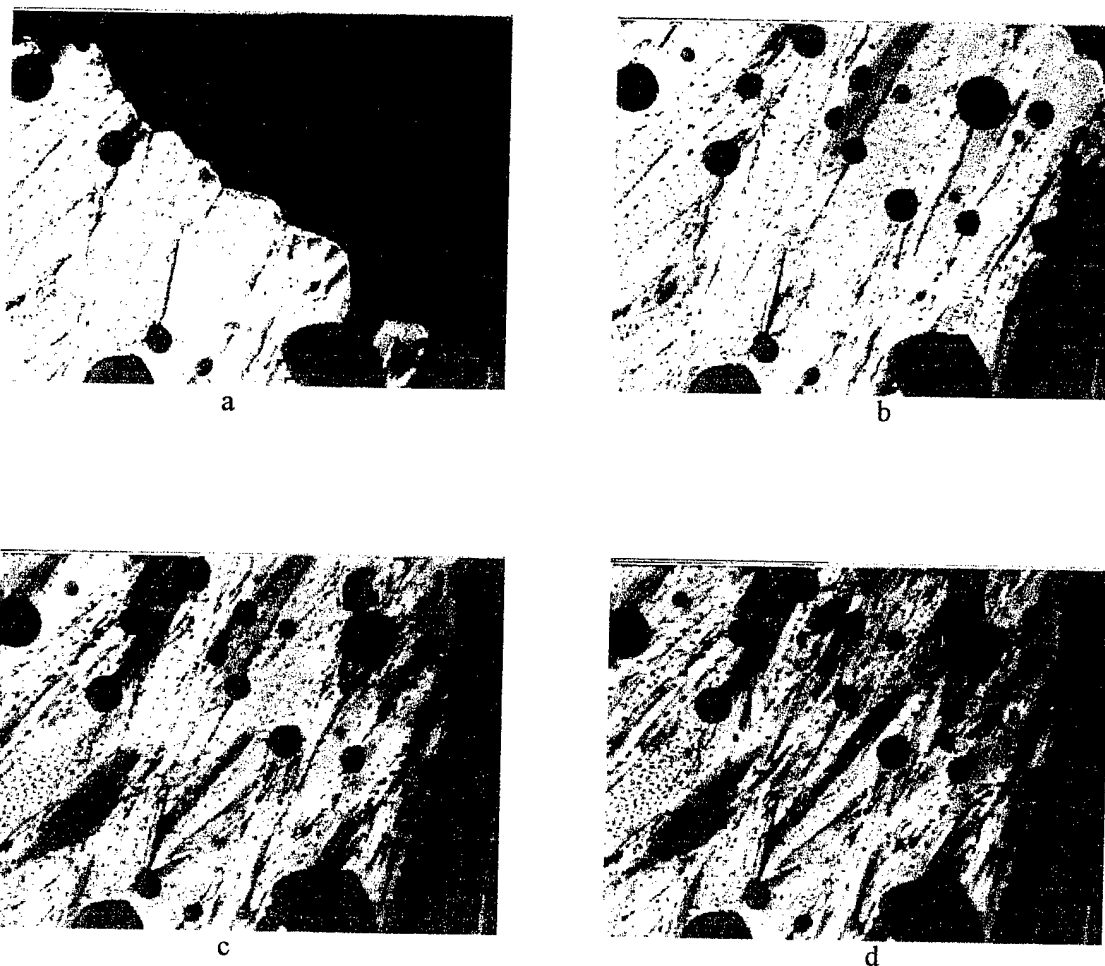Figure 5. Solid-solid transition from **TNDAZ (I)**annealed to **TNDAZ (II)**

Figure 6. (a) Continuous, irregular crystal front of **TNDAZ (I)** at 127.8 °C, (b) thin crystalline film of **TNDAZ (I)**, (c) spontaneous transition from **TNDAZ (I)** to **TNDAZ (II)**, (d) thin crystalline film of **TNDAZ (II)**
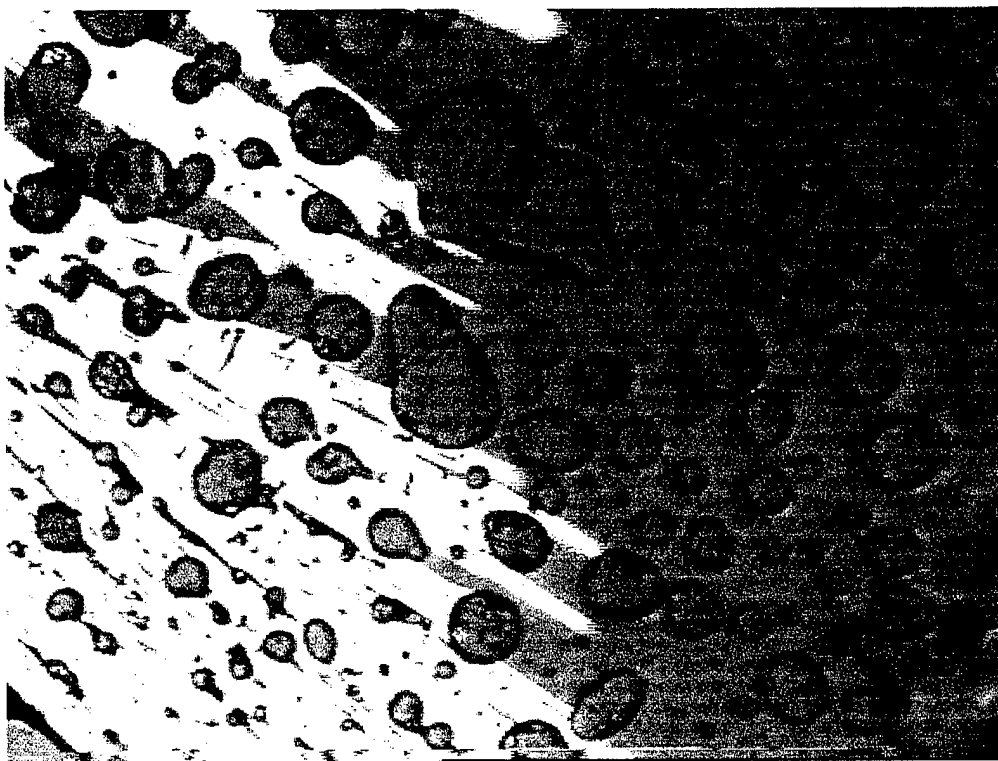
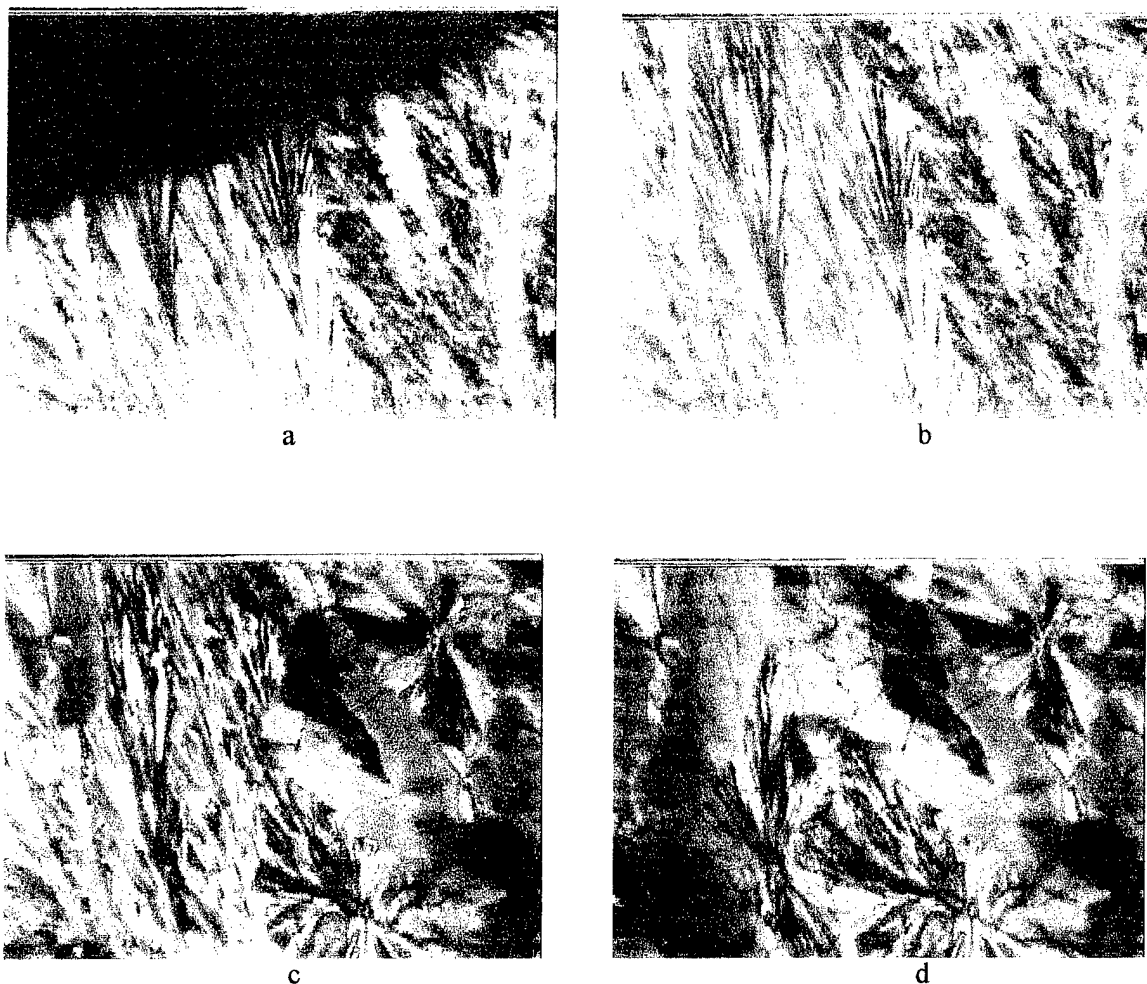Figure 7. Flattened rod crystal front of **TNDAZ (II)** at 150 °C

Figure 8. (a) Crystal front associated with the crystallization of liquid **TNAZ (II)** at 46 °C, (b) thin crystalline film of **TNAZ (II)**, (c) spontaneous transition (r to l) of **TNAZ (II)** to **TNAZ (I)** , (d) thin crystalline film of **TNAZ (I)** with macro-shrinkage cracks
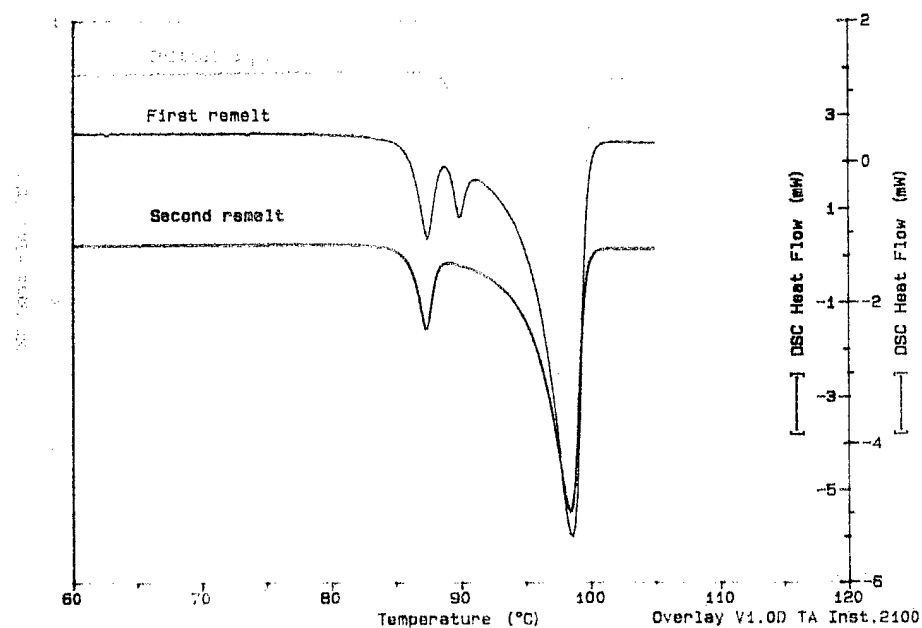
Figure 9. Composite DSC thermogram showing the initial melting and the polymorph influenced first and second remelting endotherms associated with the binary mixture containing 96.7 mol percent **TNAZ**

Figure 10. Fine-grained **TNAZ/TNDAZ** eutectic composition shown in the zone of mixing
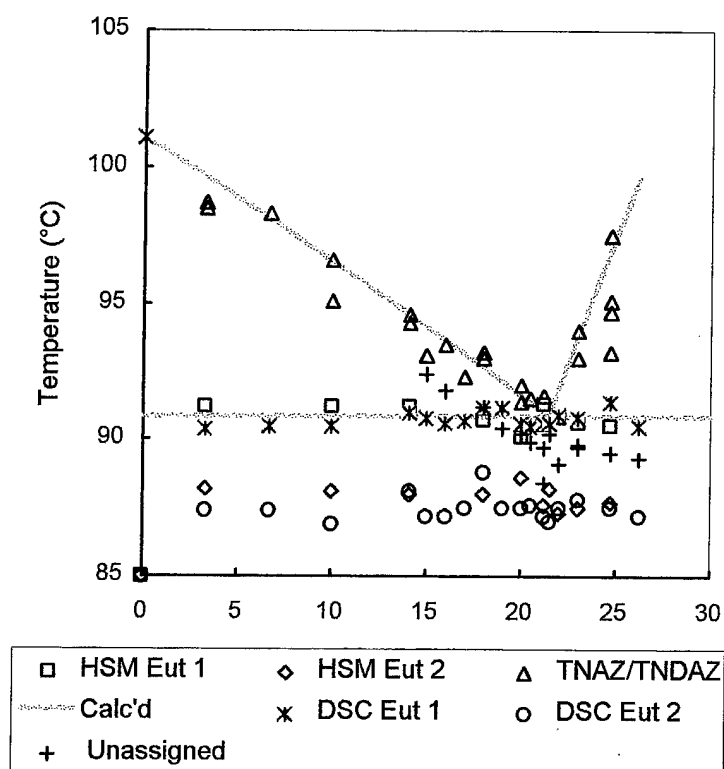
31

Figure 11. Calculated phase diagram for the **TNAZ/TNDAZ** system with supporting experimental data
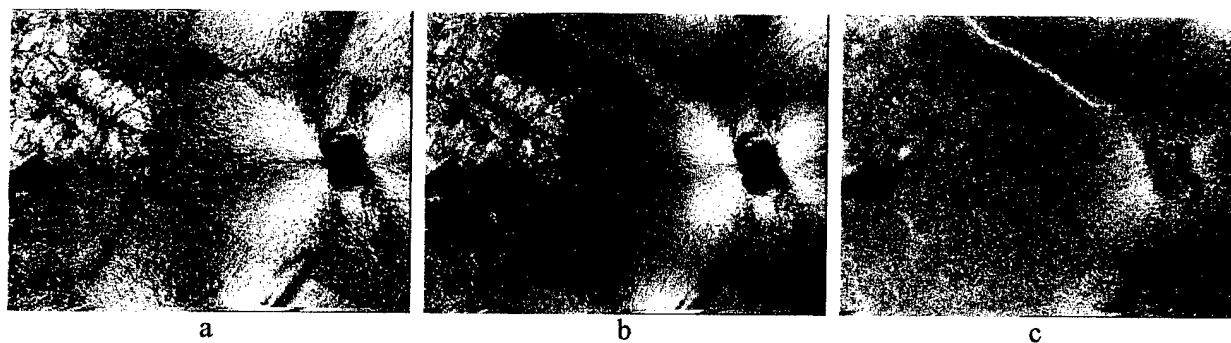

Figure 12. Surface texture change/darkening observed when a **TNAZ/TNDAZ** mixture containing 85.9 mol percent **TNAZ** is heated from (a) 27.0, (b) 63.0 to (c) 77.2 °C
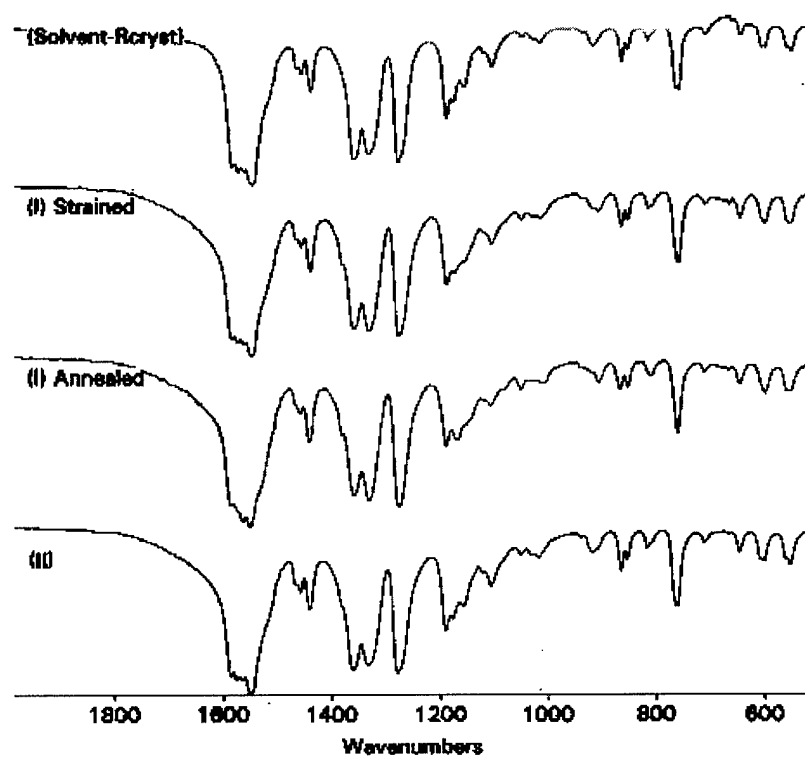
Figure 13. FTIR spectra of **TNDAZ (I)** strained and annealed, **TNDAZ (II)** and solvent recrystallized **TNDAZ**

APPENDIX A
INFRARED SPECTRAL DATA

Table A-1. Infrared Spectral Data (cm^{-1})

2[1,2]	3[3,4]	4[1,2]	TNDAZ[1,5]	TNAZ[1,5,6]
2982 (w)	2970 (s)	2975 (m)	3032 (w)	3038(w)
2968 (m)	2879 (w)	2884 (w)	3011 (w)	3022 (w)
2772 (s)	1547 (s)	1546 (s)	2976 (w)	2976 (w)
2555 (s)	1471 (w)	1481 (m)	2960 (w)	2969 (w)
1543 (m)	1361 (s)	1363 (m)	2907 (vw, br)	2917 (vw, br)
1352 (m)	1273 (w)	1233 (m)	1586 (s)	1602 (s)
1217 (m)	1234 (m)	1017 (w)	1576 (s)	1596 (s)
1125 (w)	1085 (s)		1566 (s)	1590 (s)
853 (w)			1549 (s)	1586 (s)
			1468 (w)	1544 (s)
			1459 (w)	1523 (s)
			1441 (m)	1428 (s)
			1362 (s)	1367 (m)
			1335 (s)	1342 (m)
			1281 (s)	1335 (s)
			1192 (m)	1331 (s)
			1179 (m)	1277 (s)
			1159 (w)	1220 (s)
			1107 (w)	1184 (m)
			1018 (w)	1175 (m)
			942 (vw)	1116 (m)
			920 (w)	1089 (m)
			868 (w)	1061 (w)
			855 (w)	868 (m)
			821 (vw)	843 (s)
			762 (m)	763 (s)
			604 (w)	714 (w)
			556 (w)	666 (m)
				604 (m)
				545 (m)
				528 (m)

1. KBr.
2. Nicolet Model 20SXB FTIR Spectrometer.
3. MIDAC high-resolution FTIR Spectrometer.
4. Neat.
5. Mattson Cygnus 25 FTIR Spectrometer.
6. Reference material.

DISTRIBUTION LIST
(WL-TR-96-7046)

Defense Technical Info. Center	1	WL/MNOI (STINFO Facility)	1
Attn: DTIC-OCC		WL/MN	1
8725 John J. Kingman Road, Ste 0944		WL/CA-N	1
Ft. Belvoir, VA 22060-6218			

Eglin AFB Offices:
WL/MNME   25

Commander
U.S. Army
Armament RD&E Center
Attn: R. Surapaneni (AMSTA-AR-AEE-W)
Bldg. 3022
Picatinny Arsenal NJ 07806
2

Director
Department of Energy
Los Alamos National Laboratory
Attn: M. Hiskey
P.O. Box 1663, MS C920
Los Alamos NM 87545
2

Commander
U.S. Navy
Naval Air Warfare Center
Attn: R. Chapman (Code 474220D)
China Lake CA 93555-6001
1

Commander
U.S. Navy
Naval Research Laboratory
Attn: T. Russell (Code 6110)
Bldg 207 Rm 316
Washington DC 20375
1